Science and Engineering Research Council
Rutherford Appleton Laboratory
CHILTON, DIDCOT, OXON, OX11 0QX

RAL 86-070

The Influence of Multiple Scattering on the Inelastic Neutron Scattering Spectra of Molecular Vibrations

P S Goyal, J Penfold and J Tomkinson

July 1986

THE INFLUENCE OF MULTIPLE SCATTERING ON THE INELASTIC NEUTRON SCATTERING SPECTRA OF MOLECULAR VIBRATIONS

by

P S Goyal[+]
J Penfold
J Tomkinson

Rutherford Appleton Laboratory
Chilton
Didcot
Oxon
OX11 0QX

[+] on attachment from

Nuclear Physics Division
Bhabha Atomic Research Centre
Bombay 400 085
India

Abstract

Recent results from the inelastic incoherent neutron scattering spectra of hexamethylene tetramine obtained on a new neutron spectrometer, TFXA, are reported. It is shown that the relative intensities of molecular inelastic bands, amongst themselves, are to first order unaffected by the scattering strength of the sample. As the sample scattering strength increases some slight degradation in the spectral quality occurs, and this is more apparent at higher energy transfers. These effects are related to the factors controlling momentum transfer on this type of spectrometer. It is suggested that sample scattering strengths in considerable excess of those usually allocated could be used in future for similar experiments.

I Introduction

In neutron spectroscopy the point of departure for interpretation is the well known scattering law, $S(\underline{Q},\omega)$. It is generally held that neutrons which undergo more than one scattering in the sample complicate spectral analysis, which is usually done in terms of the one phonon approximation [1]. Three fields of neutron scattering have been influential in the development of our understanding of multiscattering. These are; the dynamics of liquids [2-5], the dynamics of solids [6], and also "low Kappa" methods for the study of vibrational spectroscopy [7]. In each of these fields multiple scattering has been a problem and methods have been developed to reduce its influence.

These methods can be classified under two general headings: initially, "experimental" methods and ultimately, "correctional" methods. Thus low scattering strength samples are investigated. Typically the samples scatter only 10% of the incident neutrons. These samples may be provided with internal absorbing plates to discriminate against unwanted scattering vectors. If these experimental methods are inapplicable, or unsuccessful, recourse can be had to the calculation of detailed corrections. In this context the use of Monte Carlo programs [5,8] or calculations after Vineyard [1-4] may be attempted. Such calculations require some reasonable estimate of the $S(\underline{Q},\omega)$. This is especially true of those scattering laws that show continuity in energy, ω, e.g. the study of the dynamics of liquids. If the data is discontinuous (i.e. the study of vibrational modes) the final corrections are usually insensitive to the form of $S(\underline{Q},\omega)$, and so its initial estimate. In this latter case however multiple scattering events must not significantly change the magnitude of the neutron momentum transfer vector $\underline{Q}$. In spectrometers with small final neutron energies the value of $\underline{Q}$ is insensitive to the scattering angle but is determined principally by the energy of the mode being studied, provided that this is of significant energy transfer. Such spectrometers are therefore ideally suited to the study of vibrational modes.

In this paper we report results obtained from hexamethylene tetramine over a wide range of sample scattering strengths. We shall show that, to first order, there are no differences between the derived scattering laws. Therefore present spectrometer count rates can be immediately increased with no attendant degradation in spectral quality.

II Multiple scattering theory

In general for strong scattering samples, neutrons will emerge after several scattering events. Such processes are very difficult to model and we shall limit ourselves to the study of the intensities of first and second order scattering; I_n, n = 1,2. The function I_2 has contributions from three distinct sources, namely, double elastic events, double inelastic events, and elastic-inelastic events. Although I_2 should not have strong contributions from double inelastic events it is not clear, a priori, that the relative intensities of inelastic bands will be unaffected by multiple scattering. Such effects might be anticipated because of the different proportions of elastic-inelastic to inelastic-elastic events (sic).

The geometry of the experiment is described as follows; the sample is taken to be an infinite slab of thickness, t. A well collimated beam of neutrons of wave vector $\underline{k}_0$ and a uniform current density I_0 neutrons per cm^2 per steradian per second is incident along a direction normal to the surface of the sample. The wave vector of neutrons that emerge from the sample and proceed towards the analyser is $\underline{k}$. This makes an angle $\theta(=135°)$ with the slab normal. The scattering law of the sample is taken to be a series of delta functions. Let us assume that two scattering events occur at A and B respectively. The incident neutron is first scattered at A when it changes its energy from E_0 $(=\hbar^2k_0^2/2m)$ to E' $(=\hbar^2k'^2/2m)$ and proceeds along $\underline{k}'$. In second scattering at B it changes its energy from E' to E $(=\hbar k^2/2m)$ and emerges from the sample in the direction of $\underline{k}$. Where $\hbar\underline{Q}_1$ $(= \underline{k}' - \underline{k}_0)$ and $\hbar\underline{Q}_2$ $(= \underline{k} - \underline{k}')$ are the momentum transfers and $\hbar\omega_1 = E' - E_0$ and $\hbar\omega_2 = E - E'$ are the energy transfers at the two scatterings respectively. The trajectory of the neutron can be described using a spherical co-ordinate system with its pole along the inward slab normal. The vectors $\underline{k}_0$, $\underline{k}$ and the slab normal are coplanar and the azimuthal angle ϕ is measured from this plane. The directions of $\underline{k}_0$, $\underline{k}'$ and $\underline{k}$ are given by polar angles (0,0), (θ', ϕ') and $(\theta, 0)$ respectively. At first scattering, neutrons can be scattered in any direction (i.e. θ', ϕ' can take any value) within the sample, the scattering angle will be θ'. With a given (θ', ϕ'), for neutrons to emerge in direction (θ, ϕ) after second scattering, the scattering angle at second scattering should be β such that

$$\cos\beta = \cos\theta'\cos\theta - \sin\theta'\sin\theta\cos\phi \qquad (1)$$

Using a method developed by Vineyard and later workers [2-4,9] it can be shown that the first and second order scattered currents I_1 and I_2 are given by

$$I_1(Q,\omega) = I_0 \sqrt{\frac{E}{E_0}} \frac{N\sigma_s}{4\pi} \frac{\sec\theta[1 - e^{-(\mu_0 - \mu\mathrm{Sec}\,\theta)t}]}{[\mu_0 - \mu\mathrm{Sec}\,\theta]} S(Q,\omega) \qquad (2)$$

$$I_2(Q,\omega) = I_0 \sqrt{\frac{E}{E_0}} \frac{N\sigma_s}{4\pi} \int dE' \int_0^{\pi} \sin\theta' d\theta' F(\theta,\theta') \int_0^{2\pi} S(Q_1,\omega_1)S(Q_2,\omega_2)d\phi \qquad (3)$$

where μ_0, μ' and μ are the total macroscopic cross sections for the samples at neutron energies of E_0, E' and E respectively. Also $\hbar Q(=\hbar Q_1+\hbar Q_2)$ and $\hbar\omega(=\hbar\omega_1+\hbar\omega_2)$ are the total momentum and energy transfers after two scatterings.

In the above expressions, N is the number of scattering centres per unit volume of the sample and σ_s is the bound atom scattering cross section of the scattering nuclei. $S(Q,\omega)$ is the scattering law of the sample. The functions $F(\theta,\theta')$ correspond to $f_\varepsilon(\theta,\theta')$ in reference 3.

Multiple scattering calculations were produced for idealised spectra. These were taken to have an elastic component and three inelastic bands. The total scattering I_T $(=I_1 + I_2)$ was calculated in the region of these peaks for various thicknesses. These calculations are compared with results later. We assume that the neutron scattering can be described by a scattering law of the type:

$$S(Q,\omega) = [\delta(\omega)\, e^{-Q_0^2 \langle\tilde{U}^2\rangle} + \sum_{i=1}^{3} Q_i^2 \langle\tilde{U}_i^2\rangle\, e^{-Q_i^2 \langle\tilde{U}^2\rangle}\, \delta(\omega-\omega_i)] \qquad (4)$$

where

$$\langle U_i^2\rangle = \frac{h}{M_i \omega_i}$$

and

$$\langle \tilde{U}^2 \rangle = \sum_{i=1}^{m} \langle U_i^2 \rangle$$

Here Q_0 and Q_i's stand for the wave vector transfers corresponding to the elastic and inelastic peaks. M_i and ω_i are the effective mass and the vibrational frequencies of the i'th oscillator. Three oscillator frequencies were selected as being representative of the spectrum, they were chosen at energy transfer 5.2 meV, 47 meV and 64 meV. The total scattering I_T (= I_1 + I_2) of the thinnest sample (t = 0.13 cm), for several values of the masses, M_i was calcualated. These calculations require a knowledge of the total cross-section σ_T. We have used, σ_T = 710 barns/molecule. This value of σ_T was obtained from our transmission measurements. The transmission measurements (see experimental section) also showed that σ_T does not vary with energy in the energy region of interest. The calculated I_T reproduces the measured spectrum with M_1 = 115, M_2 = 46 and M_3 = 48. (We regard these values as parameters of the model scattering law and do not give them physical meaning.) This model of the scattering law was used to compute I_T for the other thicknesses.

III Experimental

(a) The Spectrometer

The neutron inelastic incoherent scattering (NIIS) spectrum was obtained on the inverse geometry time focused crystal analyser spectrometer (TFXA) on the spallation neutron source ISIS, at the Rutherford Appleton Laboratory, UK.

The spectrometer has been constructed with a time focusing geometry [10] which is described in detail elsewhere [11]. Energy analysis is provided by two pyrolytic graphite crystals, set at a mean backward scattering angle of 135°. The combination of the time focusing and separate energy sorting of the BF_3 gas detectors provides good energy transfer resolution from a few millielectron volts (meV) energy transfer to several hundred meV. The elastic resolution is ~ 300 μvolts. Energy calibration is

obtained from the relative positions of the elastic line and known inelastic features of some standard samples [11]. The uncertainty in energy transfer, ΔE_T, is $\Delta E_T/E_T \sim 2\%$ upto energy transfers of 500 meV. The momentum transfer shows little variation from detector to detector and is a function of the energy transfer; $Q^2(\text{Å}^{-2}) \sim E_T(\text{meV})/2$.

At energy transfers greater than a few meV ΔE_T is dominated by the uncertainty in the flight path of the neutrons; the major component being the effective detector thickness (nominal physical size ~ 2.54 cms). Therefore any variations in typical sample size and effective thickness due to multiple scattering events are expected to have only a nominal effect on resolution.

(b) Transmission measurements

A 1 mm thick cadmium mask with a central hole, 10 mm diameter, was mounted behind the sample. Spectra in monitor M_2 (placed after the sample) were recorded first with the sample and then with the empty can in the beam. These spectra were normalized with respect to the incident spectrum. The transmission as a function of neutron energy was obtained from the ratio of the normalized spectra. This procedure was checked against a more conventional transmission measurement. In this case a pencil ray of neutrons (1 mm in diameter), of λ = 1.0 Å, was transmitted through the thickest sample. The results of the two measurements produced the same transmission value at 1 Å.

(c) Sample Preparation

Hexamethylene tetramine (HMT), "gold label", was obtained from the Aldrich Chemical Co, London; and used without further purification. Measurements have been made for sample thicknesses of 0.13, 0.19 and 0.54 cm. These samples incoherently scatter 17%, 24% and 54%, respectively, of the incident neutron beam, calculated at 25 meV (σ_H (25 meV) = 35 barn, [14])

(d) Data Analysis

All the spectra were normalised to the incident monitor spectrum, transformed to the scattering law, $S(Q,\omega)$ and to an energy transfer scale in meV.

IV Results and Discussion

The individual $S(Q,\omega)$ of the HMT sample (17K) are shown in Figure 1. They are consistent with previously published spectra [12] . We see immediately that the spectra are self consistent, i.e. there are no new bands in the spectra of thick samples compared with those from the thin sample. What is observed is that the total detected number of counts per energy division is dramatically increased. This overall increase can be emphasised by calculating a ratio of the different scattering laws. This is the ratio, $R(\omega)_d$

$$R(\omega)_d = \frac{S(Q,\omega)_d}{S(Q,\omega)_{0.13}}$$

where d is the thickness. The functions $R(\omega)_d$ are shown in Figure 2 for the thicknesses .19 and .54 cm. Also shown on the same figure is the spectrum for the thinnest sample. The general increase in the signals is seen to be 1.4 and 3.2 respectively.

The first ratio function, $R(\omega)_{0.19}$, is quite flat and unstructured. Thus demonstrating that sample scattering strengths up to 25% provide spectra which are true representations of the single scattering spectra. Conventional wisdom from other neutron scattering techniques would indicate that this is unusual. The apparent contradiction is resolved when it is realised that the results are related to the spectrometric method.

In inelastic spectrometers with low final neutron energies the momentum transfer vector is determined by the vibrational mode being investigated (i.e. the energy transfer). At significant energy transfers, above say 40 meV, it is irrelevant at what angle the first scattering event occurs. Therefore after first scattering early within the sample all subsequent elastic scattering events do not influence the derived scattering laws. (This is simple multiple scattering). Moreover by working with the sample in reflection both scattering processes can achieve their saturation limit.

The effect of two inelastic scattering events becomes important as the sample thickness increases. Such contributions occur in those regions of ω where the density of oscillator states is significant. We should expect this to be visible in the 0.54 cm thick sample (54% scattering). Inelastic scattering from a vibron, followed by another inelastic scattering event (vibron or phonon), will give rise to structure in $R(\omega)d$. Thus at $\omega \sim 45$ meV, where $R(\omega)_{0.54} \sim 2$ one of the two scatterings was probably an elastic event. Whereas in the region of $\omega \sim 60$ meV, $R(\omega)_{0.54} \sim 3.2$ and the increase from 2 to 3.2 has a substantial contribution from two inelastic events. The first gap in the density of states is above the external modes and below the internal modes, and corresponds to the observed "dip" at ca 40 meV in $R(\omega)_{0.54}$. A second, less depleted gap occurs at about 95 meV [12]. Therefore the continued increase in detected flux as sample strength increases, is due to those neutrons which excite firstly an internal vibration and subsequently excite another vibration, either a phonon or a vibron (this is multiple phonon scattering). This should not be confused with single scattering events that generate several phonons; multi phonon scattering.

It can be seen that the thickest sample does not produce the same spectral quality as the thinnest sample. This spectral degradation is more apparent for the high energy transfer region. This undoubtedly results from the multiple phonon scattering. Neutrons are being detected at energies removed from the vibron transition energy. However this degradation is never so bad as to reduce the spectrum, even of the thickest sample, to noise.

We have also investigated the influence of scattering strength on the observed width of spectral bands. The intense feature at 47 meV is a good candidate for this investigation. This band is assigned to ν_{16}, a deformation mode of the carbon-nitrogen skeleton. The width of the ν_{16} band in HMT is the narrowest reported for an NIIS spectrum, 11.5 cm^{-1} [12]. Our spectra from the samples of different scattering strengths were normalized at their peak heights and overplotted. This is shown in Figure 3. It is seen that there is no dramatic increase in band width. Rather a slight broadening at the base. The subtraction of two normalised spectra (strongest minus weakest) is also shown in Figure 3. Here the differences at the base have been strongly emphasised. We may conclude that to first order the widths of spectral bands are independent of scattering strength.

The natural width of ν_{16} band can be estimated by removing the instrumental contribution. The instrumental width, $\Delta\omega$, in this spectral region is calculated to be $\Delta\omega = 6.8\ cm^{-1}$. The measured bandwidth, FWHM (for d = 0.13) $\Delta\omega_{\nu 16} = 8.3\ cm^{-1}$. Therefore the natural width of this band $\Delta n_{\nu 16}$, can be estimated to be $\Delta n_{\nu 16} \sim 4.8\ cm^{-1}$.

Although the $R(\omega)$ function is flat, for $\omega > 100$, the individual spectra appear above a generally higher level for stronger scatterers. Therefore weak, broad, features will become more difficult to differentiate in this spectral region as the sample scattering strength increases.

We shall now discuss the results of our calculations. The ratios of the calculated intensities of the selected frequencies, are shown plotted in Figure 4. Also shown in the same figure are the observed ratios. Although the number of selected frequencies was small the comparison of calculation with experiment is excellent. Only three calculated points do not fall immediately on the observed curves, and these can be explained. The first point is $R_{calc}(\nu_{25})_{0.54}$. In the observed spectrum the ν_{25} band sitting on a broad multi phonon level. Unfortunately our model of the external density of states is a delta function at $\omega_D = 5.2$ meV. If a more realistic density of states had been used the value of $R_{calc}(\nu_{25})_{0.54}$ would have been larger. The remaining two points are $R_{calc}(2\nu_{16})_{0.54}$ and $R_{calc}(\nu_{16} + \nu_{25})_{0.54}$. Because our calculations do not consider the possibility of phonon wings [13], the peak intensities fall at the zero phonon line frequency. In real systems however, especially at large Q, the principal intensity of an internal mode will be at about $\nu_i + n\omega_D$ [13]. The production of a single ν_{16} is associated with relatively low Q and hence the main intensity in weak scatters is at the zero phonon line. However the first ν_{16} vibron to be created in a multiple scattering double vibron excitation requires relatively high Q. Therefore $R_{calc}(2\nu_{16})_{0.54}$ actually corresponds to $R_{obs}(2\nu_{16} + n\omega_D)_{0.54}$, with $n \sim 2$ or 3, and the comparison again becomes excellent.

Our calculations suggest the following simple model for the change from simple multiple scattering to multiple phonon scattering. Firstly the dominant scattering process involves the excitation of a vibron.

Therefore the final energy of the neutron will be relatively low. Secondary elastic scattering process, originally insignificant for weak samples, begin to appear as the scattering strength increases. The corresponding increase in detected neutrons, is due to elastic scattering, which rapidly saturates in reflection geometry. This is because elastic scattering events are nearly isotropic, and they will diffuse those neutrons, first scattered, deep within the sample. If the scattering strength is augmented, beyond the point that second elastic events are increasing the detected counts, the increases in detected neutrons are due to second inelastic scattering.

So far in the discussion we have concentrated on understanding the role played by the scattering strength in the function $R(\omega)_d$. However, even for moderate scattering strength samples it is only necessary to consider single inelastic scattering events. This is because the relative intensities of the single and double inelastic bands, for samples of a given scattering strength, remain approximately constant. It can be seen from Table 1 that

$$R(\nu_{16})_d \approx R(\nu_{25})_d$$

and $$R(2\nu_{16})_d \approx R(2\nu_{25})_d$$

but $$R(2\nu_{16})_d > R(\nu_{16})_d$$

However a value of the scattering strength may be chosen where $R(\omega)_d \sim R(2\omega)_d$. Scattering strengths of up to 25% satisfy this criteria, and provide relative band intensities that can be adequately interpreted in terms of a one phonon scattering law.

Conclusions

The NIIS spectra of HMT for several different scattering strengths have been obtained on TFXA. The ratioed spectra were presented and detailed multiple scattering calculations were performed. We may conclude, for reflection neutron inelastic spectrometers with low final energy, that:

i) samples that scatter only 10% of the incident beam are probably inefficient. Neutrons which have been down scattered once can be scattered again, elastically, and are still well described by the one phonon approximation. Total sample scattering strengths of up to 25% are to be recommended for experiments where the inelastic bands occur at energy transfers greater than 40 meV and relative band intensities are acceptable, i.e. molecular spectroscopy.

ii) Samples that have high scattering strengths continue to show understandable increases in the detected count. These increases arise from multiple inelastic scattering.

Therefore initial experiments of a survey nature on uncharacterised samples are recommended to have scattering strengths, of ca 50%, thereby dramatically reducing the experimental time (by factors of ca 4 to 5).

iii) Degradation of spectral quality will manifest itself by a loss of structure, by weak high energy features becoming less "visible" and by all bands broadening slightly at their base.

iv) The ν_{16} (0→1) band of HMT is now reported with a natural width (FWHH) < 5 cm^{-1}.

Acknowledgements

Here we should like to thank Dr C Carlile, Dr R C Ward and AERE Harwell for producing the conventional transmission measurements. PSG would also like to thank staff of RAL for their help and hospitality during the period of his stay.

References

1. G H Vineyard, Phys Rev 96 93 (1954).

2. K R Rao, B A Dasannacharya and S Yip, J Phys C Solid State Phys 4 2725 (1971).

3. A K Aggarwal, Phys Rev A4 1560 (1971).

4. V F Sears, Adv Phys 24 1 (1975).

5. J R D Copley, Computer Phys Comm 7 289 (1974).

6. M Bee and J P Amoureux, Mol Phys 41 287 (1980).

7. K A Strong and R M Brugger, J Chem Phys 4 421 (1967).

8. M W Johnson, AERE - R7682 (1974), a report of Atomic Energy Authority, Harwell, UK.

9. P S Goyal, J S King and G C Summerfield, Polymer 24 131 (1983).

10. S Ikeda, N Watanabe and K Kai, Physica 120B 131 (1983).

11. J Penfold and J Tomkinson, RAL-86-019 (1986), a report of Rutherford Appleton Laboratory, Chilton, UK.

12. H J Lauter and H Jobic, Chem Phys Lett 108 393 (1984).

13. M Warner, S W Lovesey and J Smith, Z Phys B51 109 (1983).

14. "Neutronic cross sections" ed D J Hughes and J A Markey BNL 325, US Atomic Energy Commission 1955.

FIGURE CAPTIONS

Figure 1

The scattering laws determined for the different thicknesses of hexamethylene tetramine d = 0.13, 0.19, 0.54 cm, all at 17K.

Figure 2

The scattering law for HMT (d = 0.13) and the ratio functions $R(\omega)d$, for d = 0.19 and 0.54, described in the text. Also shown are two horizontal lines which intercept the absica at $R(\omega) = 1.4$ and 3.2 respectively.

Figure 3

Detail of the spectra of HMT around 47 meV neutron energy transfer, showing the normalised observations of the ν_{16} mode (see text). Also shown, below, the difference between the normalised results from the thickest and thinnest samples.

Figure 4

Comparison of the calculated $R(\omega)d$ values with the observations. The observations are enlarged from figure 2 and the calcualted points are the bold dots. The apparent failure of some of the points to correspond with observations is due to the simplicity of the model, and is explained in the text.

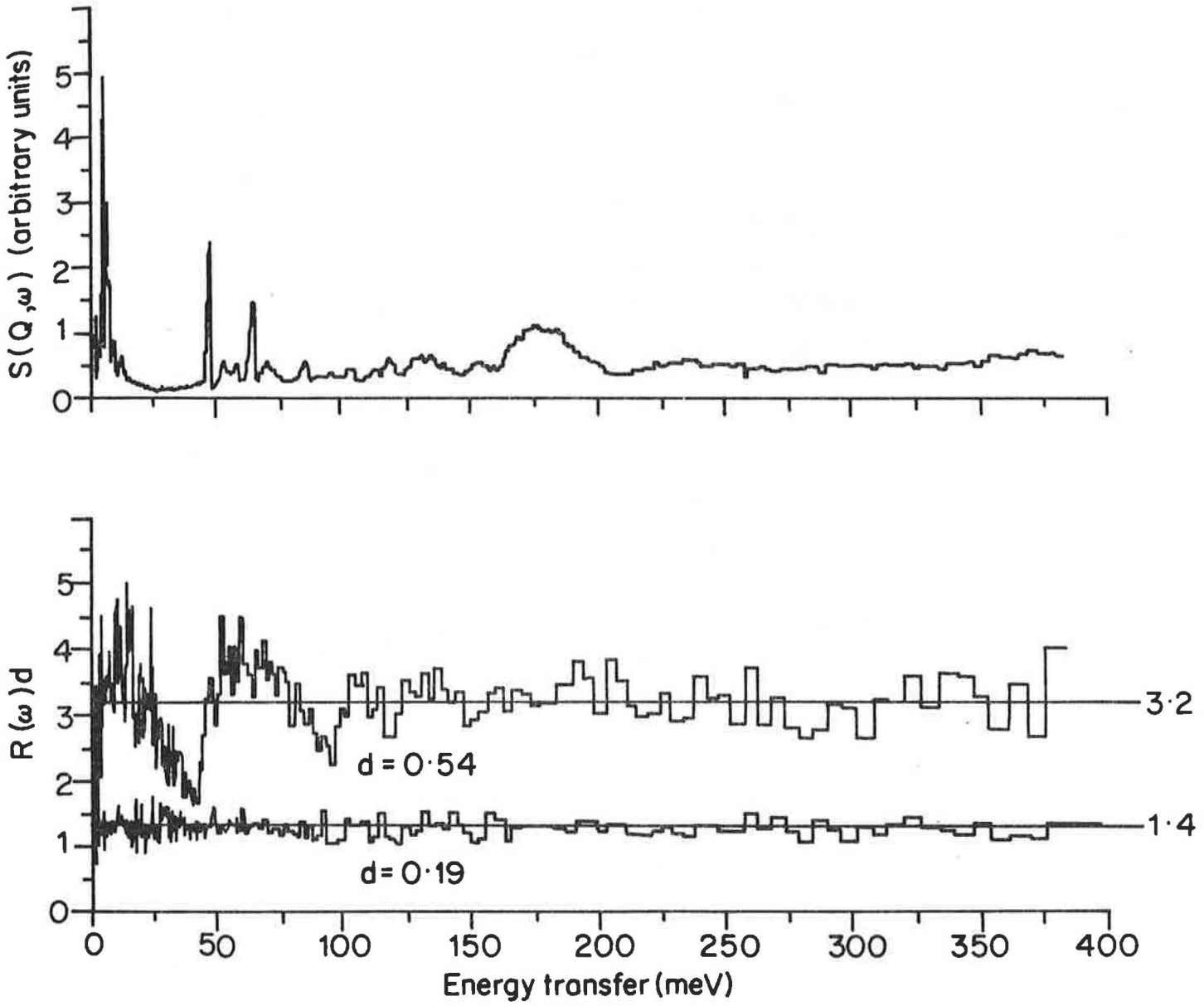
S(Q,ω) (arbitrary units)
0
1
2
3
4
5
R(ω)d
d = 0·54
d = 0·19
3·2
1·4
0
50
100
150
200
250
300
350
400
Energy transfer (meV)

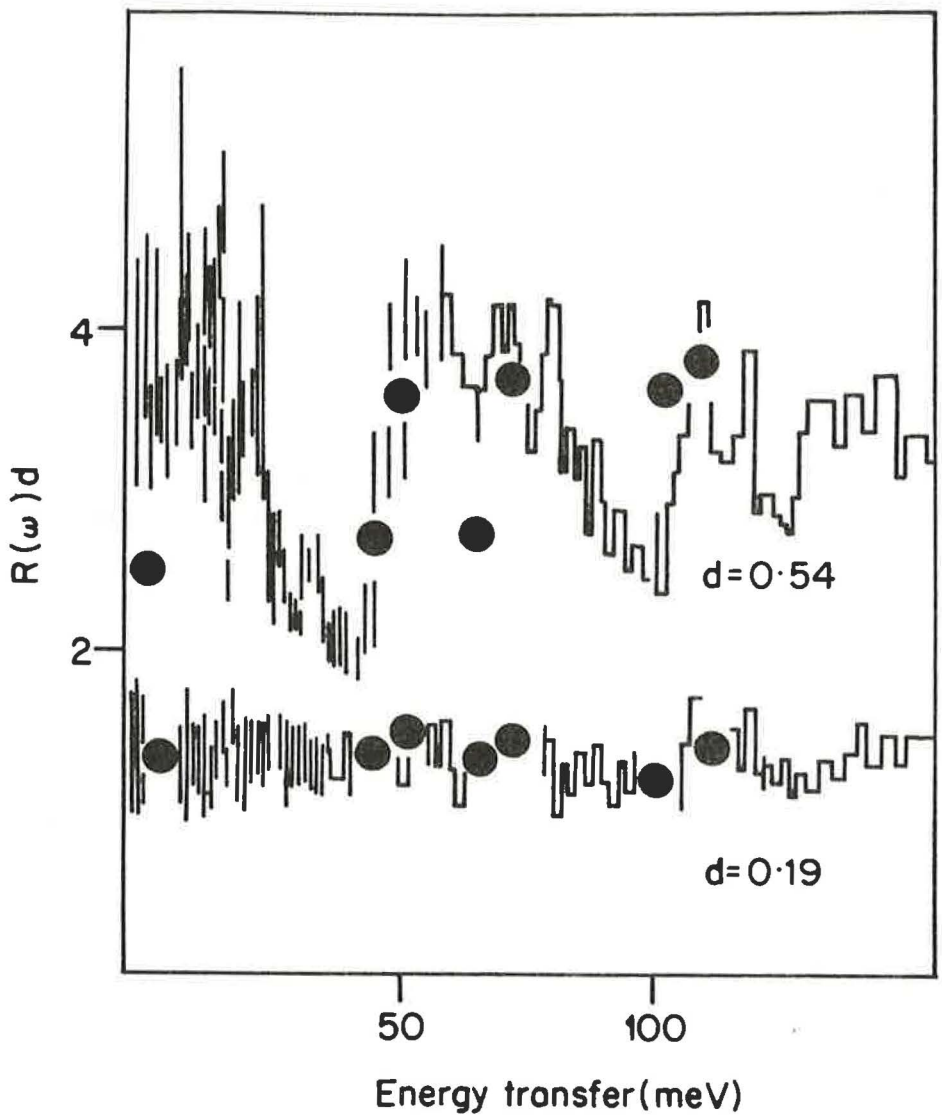
4
2
R(ω)d
d=0·54
d=0·19
50
100
Energy transfer(meV)

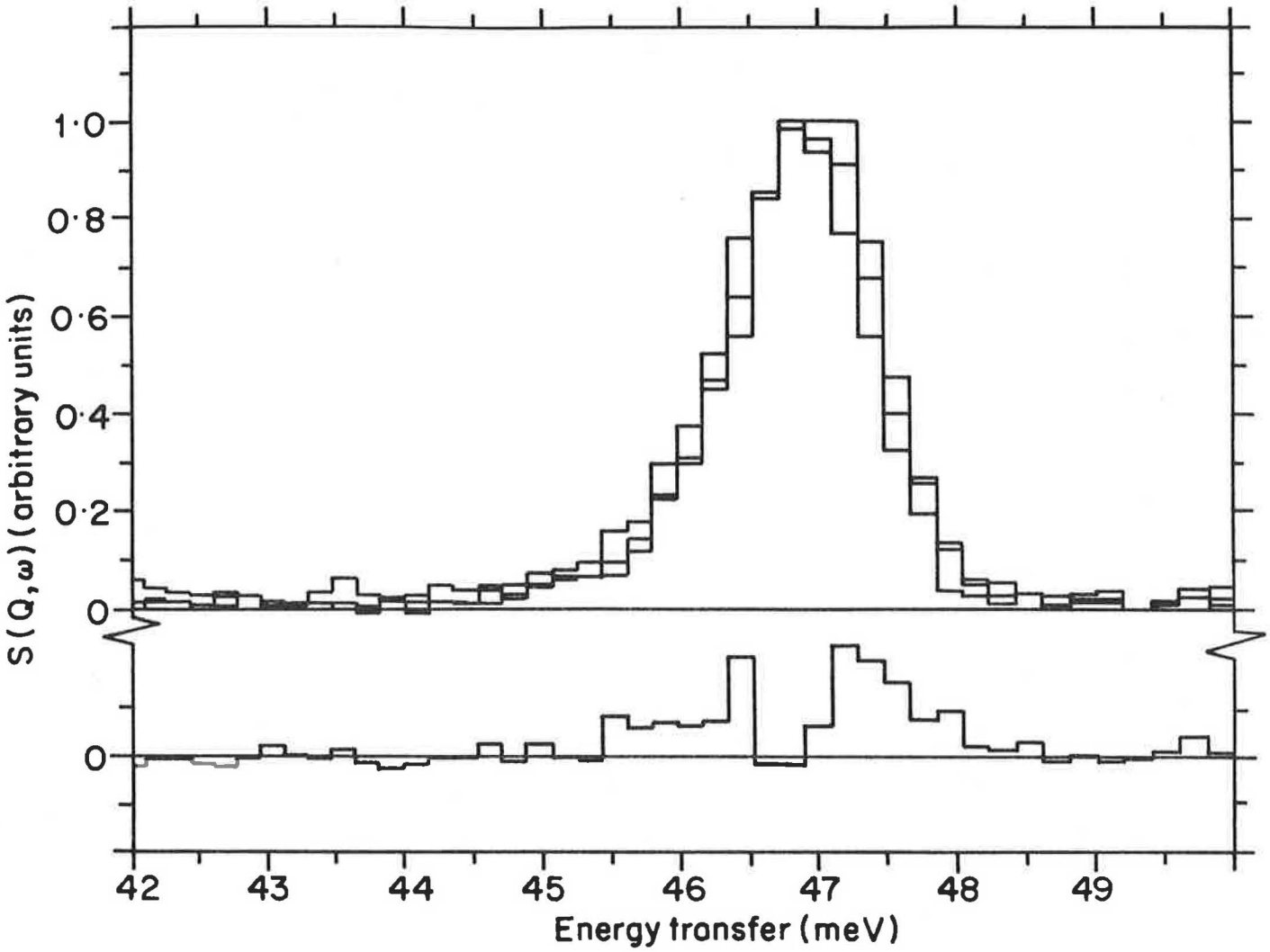
1·0
0·8
0·6
0·4
0·2
0
0
S(Q,ω) (arbitrary units)
42
43
44
45
46
47
48
49
Energy transfer (meV)

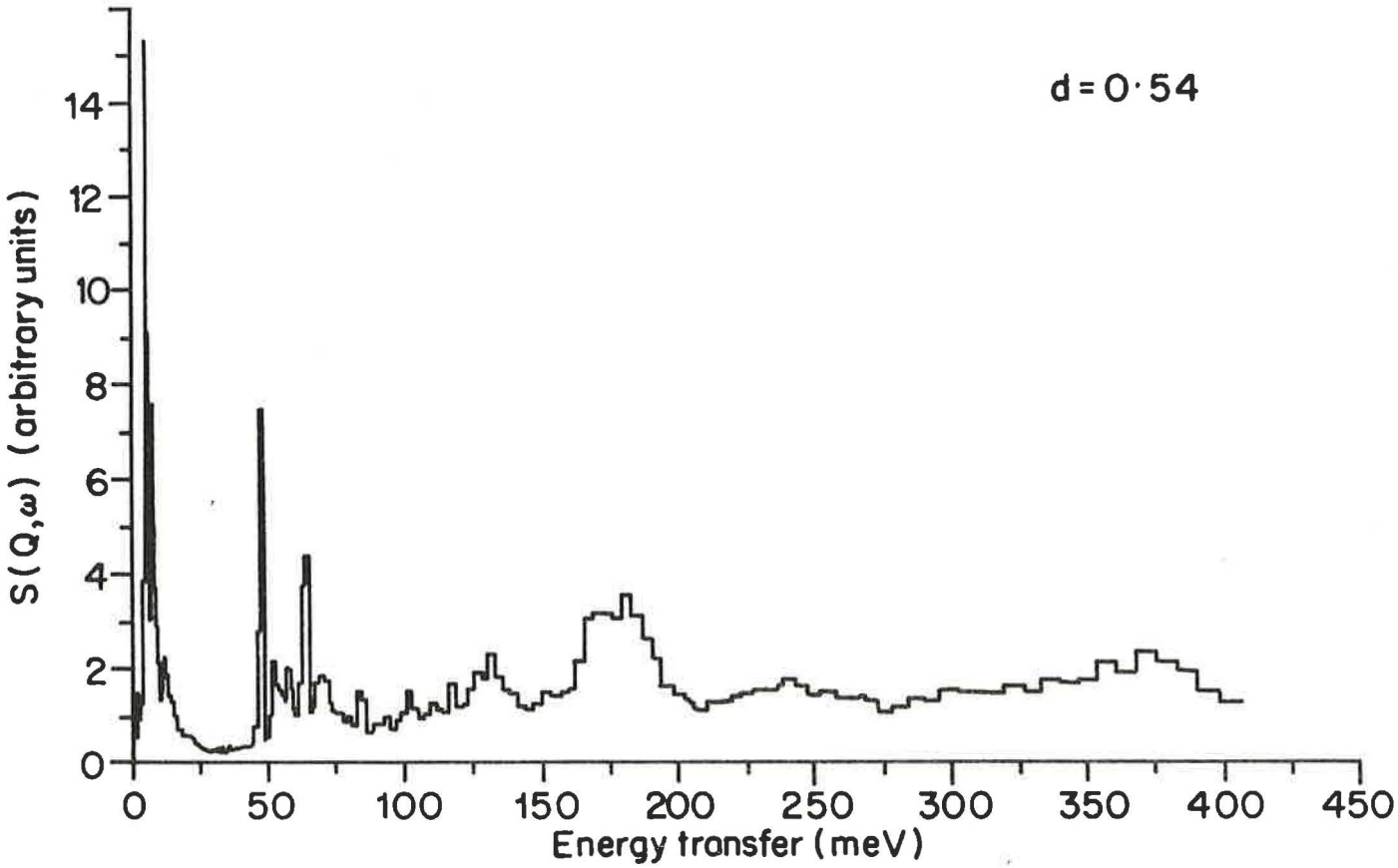
d = 0·54
S(Q,ω) (arbitrary units)
0
2
4
6
8
10
12
14
0
50
100
150
200
250
300
350
400
450
Energy transfer (meV)

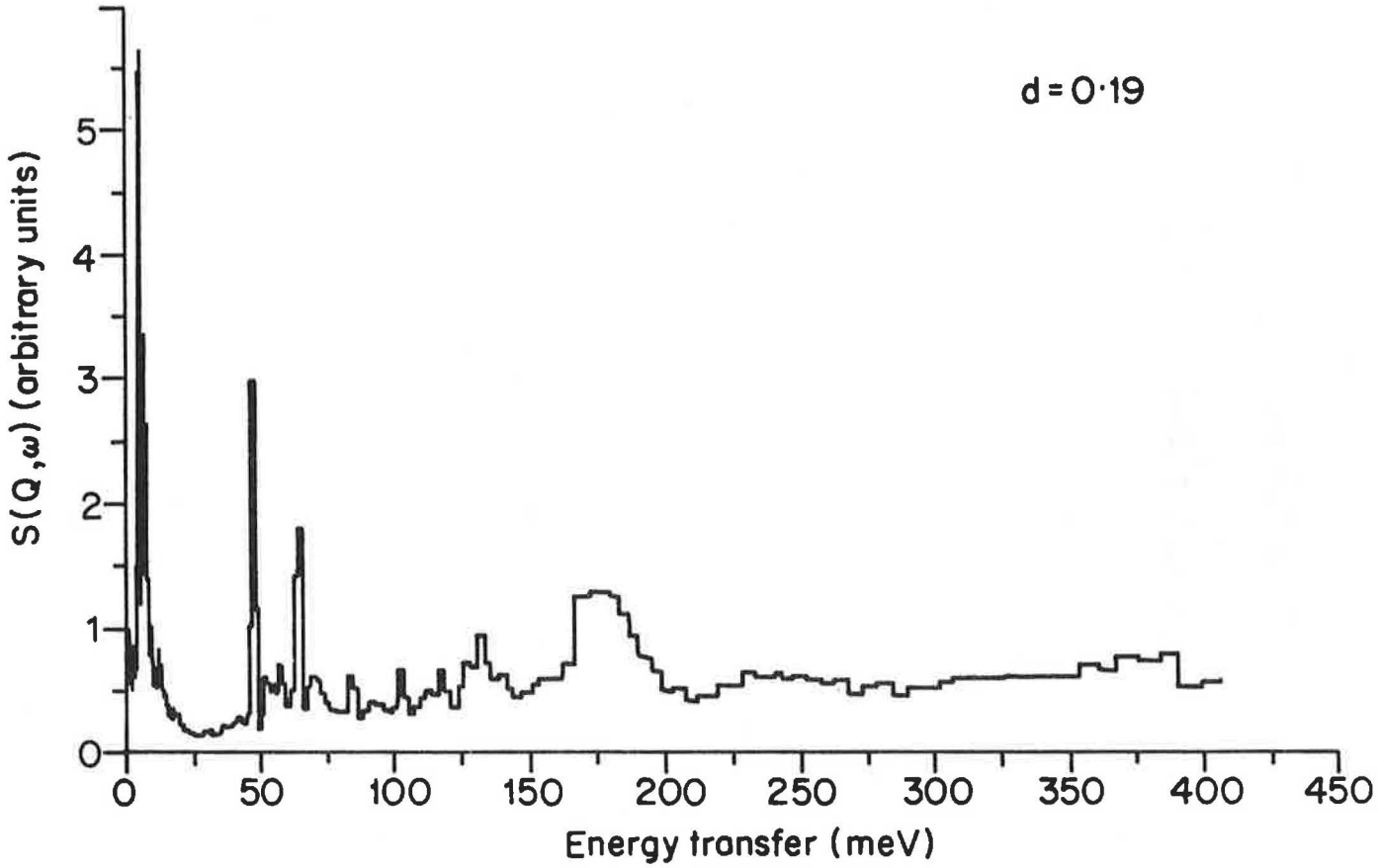
d = 0·19
S(Q,ω) (arbitrary units)
0
1
2
3
4
5
0
50
100
150
200
250
300
350
400
450
Energy transfer (meV)

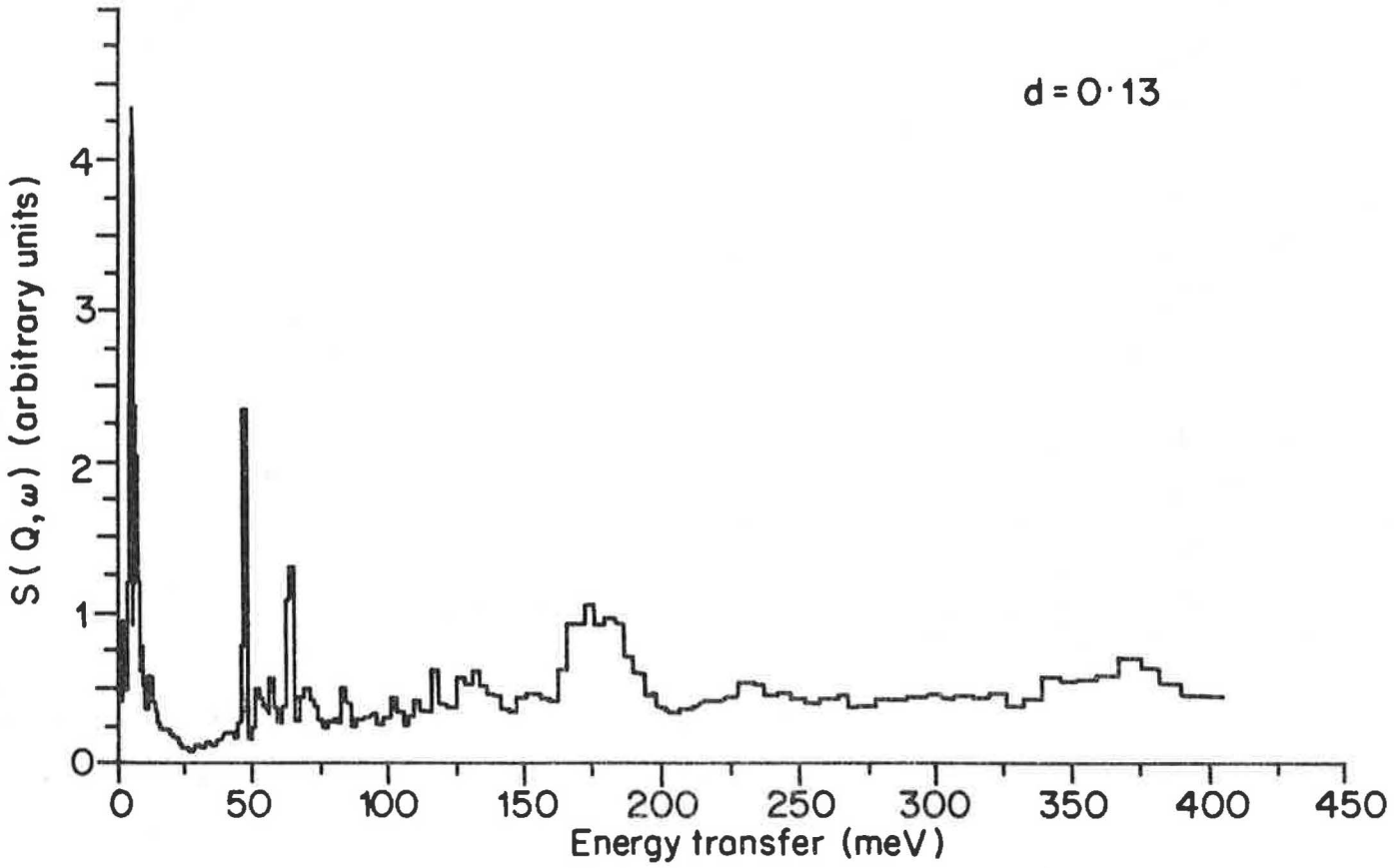
d = 0·13
S(Q, ω) (arbitrary units)
0
1
2
3
4
0
50
100
150
200
250
300
350
400
450
Energy transfer (meV)